Modeling Approach for Intumescing Charring Heatshield Materials

Gerald W. Russell*

U.S. Army Aviation and Missile Research Development and Engineering Center, Redstone Arsenal, Alabama 35898

and

Forrest Strobel[†]

ITT Industries, Huntsville, Alabama 35806

Intumescing heatshield materials have been shown to provide significant thermal protection for missile system environments. The design and use of these materials requires the analytic understanding of a considerable level of thermodynamic phenomena occurring on the surface as well as in-depth. These phenomena can include in-depth thermochemical decomposition, pyrolysis gas generation and mass transfer, thermophysical property change, thermochemical and mechanical ablation, intumescence or conduction path growth, and boundary-layer modification due to pyrolysis gas injection or surface reactions. The current state of the art for modeling thermochemically decomposing heatshield materials is enhanced through the addition of intumescent behavior effects to the Aerotherm Charring Material Thermal Response and Ablation Program (CMA). State-of-the-art real-time radiography methods along with embedded thermocouples were utilized in a radiant heating environment to obtain in-depth thermochemical decomposition, thermal response, and intumescence. The resulting intumescence model was applied and validated for a low-shear hypersonic high-altitude environment.

Nomenclature

A	=	area, in.^{2} (cm^2)
C_p	=	specific heat, Btu/lbm · °F (kJ/kg · K)
E	=	activation energy, lbf · ft/lbm (N · m/kg)
h	=	enthalpy, Btu/lbm (kJ/kg)
$\bar{h}$	=	weighted enthalpy, Btu/lbm (kJ/kg)
k	=	thermal conductivity, Btu/ft · h · °F (W/m · K)
L	=	node thickness in intumescence model, in. (cm)
LFAC	=	intumescence term (function of char state and heat rate)
m	=	mass, lbm (kg)
$\dot{m}$	=	mass flow rate, lbm/s (kg/s)
n	=	Arrhenius decomposition reaction order
P_F	=	preexponential factor, 1/s
q	=	heating rate, Btu/ft^2 · s (W/cm^2)
R	=	gas constant, lbf · ft/lbm · °R (K)
s	=	surface erosion depth or position, in. (cm)
$\dot{s}$	=	surface erosion rate, in./s (m/s)
T	=	temperature, °F (°C)
x, y	=	spatial coordinate, in. (cm)
Γ	=	resin to fiber volume fraction
θ	=	time, h
ρ	=	temperature varying density of material, lbm/ft^3 (kg/m^3)
φ	=	char state

Subscripts

c	=	char
g	=	pyrolysis gases
$0, v$	=	initial condition or virgin material

Introduction

DURING the past several years, a significant level of research and development has been applied to optimization of missile systems for performance enhancement. One of the primary methods of enhancing performance is to reduce weight, thereby increasing velocity and range. To address the weight reduction requirement, composite technology has been increasingly utilized in missile airframe design. Although these composite structures afford a significant weight reduction, they are typically limited in operating temperature. As a result, a thermal protection system is required and must be designed in an optimal manner to maintain the weight reduction achieved through the use of the composite airframe.

One of the most widely accepted methods for analysis and design of external thermal protection systems is the charring material approach,[1] in which an attempt is made to model the thermodynamic phenomena occurring throughout the material and boundary layer. This approach provides a relatively rigorous mathematical treatment of thermochemical decomposition and ablation, allowing for the identification of sensitivities to the various phenomena. This also provides a means of optimizing heatshield requirements for given geometries and aerothermal environments. Whereas this approach adds significantly to the analytic capability of modeling heatshield thermodynamic behavior, it still requires a level of empiricism due to its current inability to model the effects of intumescence (swell or expansion) on in-depth thermal response. Recent studies[2] have led to the identification of intumescing heatshield materials having significantly higher thermal performance than many of the nondecomposing and ablating materials commonly used. The phenomenon of intumescence increases conduction path length and induces additional thermophysical property changes that contribute to the reduction of in-depth thermal penetration. Figure 1 provides a schematic of the nonintumescent model compared to the new intumescent model. Figure 1 shows the various regions within the heatshield undergoing decomposition and expansion. As can be seen for the nonintumescent model, the conduction path is fixed, whereas the new intumescent model accounts for the effects of conduction path growth.

The objective of this research is to further reduce the level of empiricism through the development and experimental validation of mathematical relationships for intumescence and to incorporate these relationships into the Aerotherm Charring Material Thermal
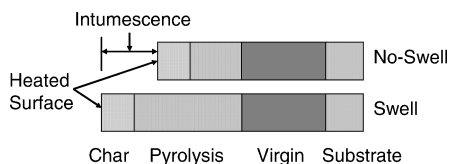
Fig. 1   Schematic of models for thermochemically decomposing heat-shields.
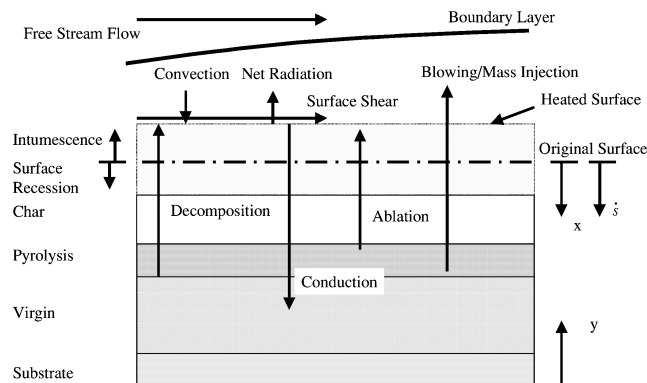

Fig. 2   Schematic of thermochemical decomposition phenomena.

Response and Ablation Program (CMA),[3] providing a means of more accurately predicting heatshield requirements and enhancing system level optimization. The approach for accomplishing the research objectives were initiated with the development of mathematical expressions for intumescence. These expressions were then incorporated into the existing thermochemical decomposition model CMA in a one-dimensional finite difference approach. Experimental data were collected through the use of a high heat flux test facility while aerodynamic shear effects were minimized. The test environment provided a controlled thermal boundary condition and allowed for in-depth decomposition to be monitored as a function of time and position through the use of real-time radiography and embedded thermocouples. The resulting model was then applied to low- and moderate-shear hypersonic convective thermal environments for which test data had been previously collected. These results provided an indication of the model accuracy in an actual freestream air environment for various levels of mechanical shear. The comparisons of predictions with test data for the convective aerothermal environments allowed for the identification of sensitivities to mechanical shear and the necessity to further enhance the analytic approach through modeling mechanical erosion.

Discussion

Thermodynamic Phenomena Overview

A schematic of the physical processes that occur for missile heatshield materials during exposure to aerothermal environments is shown in Fig. 2. It is quickly evident that a significant level of chemical reactions, mechanical interactions, and boundary-layer effects are possible during the heating and corresponding outgassing of decomposing materials. The following is a discussion of each of the parameters specifically identified in Fig. 2.

Freestream Flow

The freestream flow represents the resulting airflow over an airframe during flight. This term also represents the flow imparted over a test item during aerothermal experimentation.

Boundary Layer

The boundary layer is defined as the viscous region adjacent to a surface exposed to aerodynamic flow. The analytic modeling of boundary-layer flow is extensively discussed in Schlichting[4] and is used in this research effort.

Convective and Radiative Heat Transfer

The convection heat transfer term corresponds to the thermal effects of aerodynamic flow over an airframe. The resulting viscous dissipation within the boundary layer results in a temperature rise at the wall surface. The net radiation term defines the external radiation energy exchange between the external reservoir, possible shock-layer radiation, and the heatshield surface temperature. For the present research for missile applications, shock-layer radiation is negligible.

Chemical Diffusion/Reactions

The chemical diffusion and reaction processes are a result of gas generation from the thermochemically decomposing material being injected through the solid surface into the boundary layer. Additional reactions can occur between the solid surface and boundary-layer gas species such as the recombination of carbon or coking, within the char layer of a decomposing material. The reaction kinetics and diffusion rates are highly dependent on the freestream and injected gas components. For heatshields dominated by mechanical erosion, these rates are less important than for materials having a high level of decomposition and gas injection.

Decomposition

As a heatshield material is exposed to a sufficient level of convective or radiative heat transfer, the in-depth temperature increase induces relative levels of thermochemical decomposition. This decomposition results in pyrolysis gas generation and material density reduction that can be partially quantified through the use of thermogravimetric analysis (TGA).[5] Use of an inert medium while heating the sample eliminates the potential influence of reactions with air and represents the in-depth thermodynamic response of the decomposing material where air is not present. A brief description of the specific terms considered in the analytic heatshield model follows.

Char

The char term is defined by the fully decomposed or fully reacted heatshield material region and is quantified during TGA where no appreciable density changes occur during additional temperature rise. This region can vary significantly depending on the level of thermochemical ablation and mechanical erosion. The char layer is typically of a black, carbonaceous nature. However, the char can also be represented by a combination of a variety of nonreacting or condensed species that collect on the surface.

Pyrolysis

The pyrolysis region is defined as the layer at which the heated material is undergoing thermodynamic reactions and is bounded by the fully reacted char layer and the non-reacting virgin material. This is the region from which the pyrolysis gases are generated and percolated through the char to the boundary layer. It is also considered, for this research, the primary region where intumescence occurs and expansion of the conduction path moves the heated surface away from the substrate.

Blowing/Mass Injection

The evolving gases due to decomposition are percolated up from the pyrolyzing layers through the fully decomposed porous char layer and injected into the boundary-layer. As a result of the mass injection, the boundary-layer thickness increases, providing a potential reduction in heat transfer from the boundary-layer edge to the heated surface. Depending on the severity of the thermal environment, these gases can also react with air in the boundary layer.

Surface Recession/Intumescence

The surface recession term is defined as the mechanical or thermochemical removal of condensed species from the surface of the heatshield material. This phenomenon is highly dependent on the level of aerodynamic shear, heatshield char strength, enthalpy level, reactivity of boundary-layer gases, and surface material decomposition state. For high-speed aerodynamic heating and sufficiently

weak char layers, the mechanical shear removal typically dominates the ablation process and can greatly reduce the influence of thermochemical ablation. The current CMA code requires the use of a fail temperature to simulate mechanical erosion of char layers due to aerodynamic shear forces. Although this approach can be used, it does not represent the true physics of mechanical erosion and may be limited in applicability. The intumescence is a direct result of the internal thermodynamic decomposition, causing a range of expansion levels of the pyrolyzing material. The specific difference in the existing nonintumescing model as compared to the proposed intumescing model is contained in the ability to model the effect intumescence or swelling has on conduction heat transfer into the decomposing material. Figure 1 provided a schematic of this difference. A variety of approaches such as thermal expansion[6] and equivalent thermal properties[7] have been investigated in an attempt to model this behavior with varied success. A new approach will be presented for modeling intumescence relating the pyrolysis region expansion to the decomposition state and heating rate with the goal of more accurately capturing the thermodynamic phenomenon and relative effects on conduction heat transfer.

Existing CMA Numerical Model

Thermochemical Decomposition Model

The approach to providing a means of accurately predicting specific behavior of decomposing heatshield materials has been of great interest to missile design engineers due to the excessive heat loads of reentry and hypersonic flight. In the initial design stages with new materials, only limited data and material understanding may be available until more extensive testing and evaluation is conducted. Initial design studies can be conducted with semi-empirical procedures such as the simplified heat of ablation model (SHOA).[8] This design approach is adequate for conservative design as long as experiments can be conducted in thermal environments similar to those of flight. However, as design requirements are refined, optimization plays a more significant role in missile design. This requires refinement of thermal protection system design to minimize weight while providing increased thermal protection. To obtain this analytical refinement in design of thermal protection systems, more accurate models of the ablation phenomena are required. In response to the need for a more accurate characterization of the ablation phenomena desired for typical reentry vehicle thermal design, a significant step toward providing a more theoretical model of heatshield thermodynamic behavior was developed by Moyer and Rindal,[9] namely, the CMA. This program provides a means of modeling much of the surface thermochemistry and in-depth material response phenomena, allowing for identification of specific contributors that provide material insulative capability. However, a significant amount of thermophysical property data and material characterization are required before a thermal response model can be developed that utilizes this program. A discussion of the pertinent derivations and resulting finite difference expressions is provided in the following text.

In-Depth Energy Differential Equations

Mathematically representing the terms shown in Fig. 2, the differential equation defining the in-depth energy balance is

$$\frac{\partial}{\partial \theta}(\rho h A)_y = \frac{\partial}{\partial y}\left(kA\frac{\partial T}{\partial y}\right)_\theta + \frac{\partial}{\partial y}(\dot{m}_g h_g)_\theta \qquad (1)$$

The conservation of mass for a chemically decomposing material is defined as

$$\left.\frac{\partial \dot{m}}{\partial y}\right)_\theta = A\left.\frac{\partial \rho}{\partial \theta}\right)_y \qquad (2)$$

where mass transfer is associated with the pyrolyzing constituents percolating through the char, assuming no reaction with the char. As pointed out by Rohsenow and Hartnett,[1] the use of an Arrhenius-type fit has been found to model adequately the decomposition behavior of thermochemically decomposing materials. The expression is

written as

$$\left.\frac{\partial \rho}{\partial \theta}\right)_y = -P_F \exp\left(-\frac{E}{RT}\right)\rho_0\left(\frac{\rho - \rho_c}{\rho_0}\right)^n \qquad (3)$$

The expression for density can be defined in terms of a variety of reacting components combined to form the single material. TGA characterizes the weight loss and weight loss rate based on specific reactions occurring in the material while it is heated. The general form of the expression is

$$\rho = \Gamma \sum \rho_i + (1 - \Gamma)\sum \rho_j \qquad (4)$$

where Γ represents the volume or mass fraction of effective resin to effective reinforcement and the subscripts i and j represent the various reactions attributable to the resin and reinforcement densities, respectively. Early versions of CMA limited the decomposition process to three material constituents. However, more recent versions have incorporated the ability to model more than three reactions that can occur for the highly decomposing materials of interest for this research.

Boundary Conditions

The boundary conditions defined for the surface energy balance are shown in Fig. 3. The control volume is allowed to move with the receding surface as ablation/erosion/intumescence occurs. This movement can be either a net recession or expansion. The energy fluxes entering the control volume include the convective heating and energy due to chemical reactions. (This may be either a net positive or negative value depending on the nature of the chemical reactions.) The exiting energy terms represent the conduction and radiation.

Transformation of Partial Differential Equations

The existing CMA mathematical model is a finite differencing scheme that uses fixed node sizes. To account for surface removal, nodes are removed from the backside of the ablating material such that the nodal network is referenced to the receding surface. A transformation of the differential equations is performed from the global or fixed coordinate system to a body or moving coordinate system. This approach also allows for conservation of energy and mass. The difference form of the energy equation reduces to the conservation of mass equation when temperature and enthalpy are uniform. These finite difference equations are implicit in temperature. However, the decomposition finite difference forms are explicit in temperature. The decomposition nodal network utilizes a refinement of the thermal nodal network (called nodelets) to provide better resolution of decomposition gradients. The resolution is user defined and is based on the required level of refinement to capture density gradients through the decomposing material. The process utilized in the numerical scheme first involves the calculation of the decomposition gradients using the fixed nodal and nodelet thicknesses. Then the intumescence or nodal thicknesses are determined using the char state and heating rate obtained during the decomposition calculation. The thermal gradients are then calculated using the intumesced
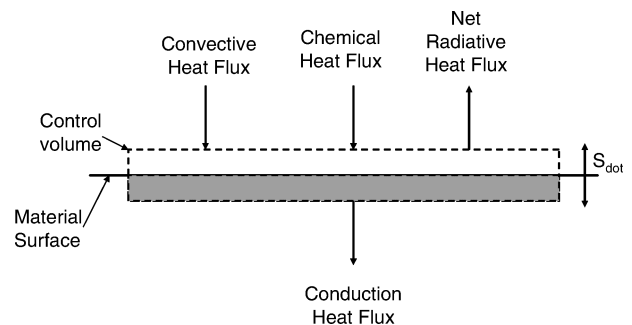

Fig. 3 Surface boundary condition schematic.

nodal thicknesses. The resulting thermal gradients are used to define the decomposition gradients for each successive temporal iteration.

The energy equation solution determines the in-depth temperature gradient and is based on intumesced nodal thicknesses. The intumescent process results in an increased conduction path and thermal resistance. This node thickness increase is only accounted for in the energy equation and not utilized in the decomposition gradient calculation. This is possible because the decomposition equation does not actually include a spatial dimension. The equations are cast in terms of density, but they are actually manipulated in terms of mass. The basic in-depth energy balance, as shown in Eq. (1), is further transformed to the moving coordinate system and results in the finite difference expression

$$\rho C_p \frac{\partial T}{\partial \theta}\bigg)_x = \frac{1}{A}\frac{\partial}{\partial x}\left(kA\frac{\partial T}{\partial x}\right)_\theta + (h_g - \bar{h})\frac{\partial \rho}{\partial \theta}\bigg)_y$$
$$+ \dot{S}\rho C_p \frac{\partial T}{\partial x}\bigg)_\theta + \frac{\dot{m}}{A}\frac{\partial h_g}{\partial x}\bigg)_\theta \qquad (5)$$

$$\bar{h} \triangleq \frac{\rho_0 h_0 - \rho_c h_c}{\rho_0 - \rho_c} \qquad (6)$$

The respective terms in Eq. (5) represents the sensible energy, net conduction, net chemical, and net convection occurring within the charring material. The conduction term containing x defines the nodal thickness modified according to the level of intumescence experienced for each node through the thickness of the material.

These expressions represent the in-depth energy balance and surface boundary conditions for decomposing materials. The nodal thicknesses along the x coordinate are fixed in the existing CMA numerical scheme. The modification discussed in the current research defines the provision for predicting transient nodal thickness or intumescence along the x coordinate.

Modified CMA Numerical Model for Intumescence

The intumescence phenomenon has been documented in a variety of analytic investigations of heatshield materials. In particular, when heatshields are used as internal insulators for rocket motors, a significant level of intumescence can occur, providing additional insulative value. Analytic modeling efforts have been performed in the past on internal motor insulation materials, such as DC93-104, where intumescence was noted. However, due to limited measurement techniques, the intumescence phenomenon could not be adequately modeled. This phenomenon was again observed during a heatshield test and evaluation program[8] in which the intumescence was such that simplified modeling techniques could not readily be used to predict heatshield thickness requirements. As a result of these analytical and experimental findings, research was directed[10] to identify a method of modeling intumescent behavior of heatshields along with validation efforts for specific environments.

The initially proposed analytic expression for modeling the intumescence as a function of char state is

$$L = \text{fnc}(\varphi) \qquad (7)$$

where L is the node thickness (as related to the x coordinate system in the numerical scheme) and φ is an expression quantifying char state. It was observed that the amount of intumescence appeared to be char state dependent and also dependent on the rate at which the material was charred. Therefore, the following relationship was adopted to model the thickness change of the material:

$$\frac{\partial L}{\partial \theta} = \frac{\partial L}{\partial \varphi}\frac{\partial \varphi}{\partial \theta} \qquad (8)$$

The char state is a function of the virgin and fully charred material defined as

$$\varphi = (\rho_v - \rho)/(\rho_v - \rho_c) \qquad (9)$$

where the subscripts v and c represent the virgin and fully charred conditions and ρ is the instantaneous density. Differentiating the char state with respect to time provides

$$\frac{\partial \varphi}{\partial \theta} = -\frac{1}{\rho_v - \rho_c}\frac{\partial \rho}{\partial \theta} \qquad (10)$$

Combining terms results in the expression for intumescence

$$\frac{\partial L}{\partial \theta} = -\frac{1}{\rho_v - \rho_c}\frac{\partial \rho}{\partial \theta}\frac{\partial L}{\partial \varphi} \qquad (11)$$

These expressions provide the basis for relating intumescence to a char state for the thermochemically decomposing material. The remaining expression, $\partial L/\partial \varphi$, must be formulated to model the actual intumescence of the material. Until additional research and development is devoted to understanding, on a microscale, the material properties that cause growth, empirical data must be used. These data must be collected during flight-similar hypersonic aerothermal test and evaluation programs in which real-time radiography of intumescence and decomposition, as well as pre- and posttest intumescence, are measured. Along with transient intumescence and decomposition measurements, in-depth temperature measurements must be collected to verify in-depth thermal response and thermal properties of the various decomposition states.

The $\partial L/\partial \varphi$ contributions to the intumescence relationship were selected utilizing a variety of analytic and experimental means. Oven tests were performed to correlate material appearance with char state. These oven tests also provided an indication of the onset and termination of intumescence for the respective heating rate. Note that these oven tests were strictly qualitative due to the differences in thermal environments and chemistry as compared to flight. However, it was noticed that discoloration for the various temperatures seen in the oven samples were similar to what was seen in the Wright–Patterson Air Force Base Laser Hardened Materials Evaluation Laboratory (LHMEL) tests with embedded thermocouples. Chemical analyses of the oven samples and LHMEL samples would provide more comparable quantitative data. The laser facility tests provided the most useful data as a result of recording transient radiography. The radiography data provided material density as a function of time and location within the test sample. This allowed for validating both char surface position and internal layer position as a function of time. These results coupled with the density measurements through the thickness as a function of time allowed for accurate predictions of in-depth thermochemical decomposition and intumescence. The embedded thermocouples provided a means of quantifying the thermal properties of the various char states. Because the thermocouple locations, density gradients, and temperatures were known as a function of time it was possible to develop a material model that could accurately predict in-depth response of the intumescing material.

It was discovered through experimental validation that the intumescence model, for the particular material of interest, was also highly dependent on heating rate. As a result, the $\partial L/\partial \varphi$ term was determined as a function of both decomposition state and heating rate to provide an approximate method of quantifying intumescence. The correlation for heating rate dependency was developed from the various aerothermal tests and imposed as a multiplier of the nonintumescing thickness. The resulting relationship to define the char state and heating rate dependent intumescence is shown in Eq. (12):

$$\frac{\partial L}{\partial \varphi} \propto \text{LFAC}(\varphi) * \text{LFAC}(\dot{q}) * L_{\text{inital}} \qquad (12)$$

for $100°\text{C/min} \leq \dot{q} \leq 20{,}000°\text{C/min}$, where LFAC is the intumescence term as a function of the char state and heating rate. This expression represents the use of multipliers for char state and heating rate effects on the initial node thickness for each time step. These multipliers are characteristic of material properties and, because they incorporate both decomposition state and heating rate, they should be applicable to a variety of aerothermal environments.

The laser test facility was utilized to isolate and quantify these intumescence properties for the analytic model. The resulting overall intumescence as defined in Eq. (12) is used in the in-depth energy balance to define conduction path length and in-depth heat transfer.

The data collected during the LHMEL tests provided the regions of intumescence as a function of char state and heating rate used to establish the $\partial L / \partial \varphi$ empirical model. The resulting multipliers generated and validated for the laser thermal testing were also used for predicting intumescence and in-depth thermal response for the NASA Hot Gas Test Facility[2] high-altitude hypersonic aerothermal testing. Predictions were in excellent agreement with posttest measured decomposition and intumescence data, as well as embedded thermocouple data for the lower shear conditions.

Intumescent Material Description

Overview

The material investigated for this research, Firex RX2390 (Ref. 11) was selected due to its highly intumescent behavior and exceptional thermal performance recently identified for missile applications. During heating the material experiences large levels of intumescence and, through decomposition, reradiation, and conduction path growth, minimizes the support structure temperature rise. The material is an inexpensive, sprayable, or trowelable fiber-reinforced epoxy. It functions as an intumescent (char swells) under low to moderate shear in high-temperature environments. At higher-shear conditions the char layer can be removed, and the thermal performance of the material is somewhat degraded. For the present study, the focus is on environments for which shear removal of the char layer does not occur.

Thermal Properties

Initial temperature-dependent thermal properties for RX2390 were determined by Perry et al. (see Ref. 12). During this program thermal properties were experimentally determined by Virginia Polytechnic Institute and State University (VPI) to verify the material properties provided by the vendor. Vendor data reported the room temperature conductivity and specific heat to be 0.19 Btu/ft · h · °F (0.33 W/m² · K) and 0.36 Btu/lbm · °F (1500 kJ/kg · K), respectively. However, the VPI measurements yielded different virgin material properties than the vendor supplied data, 0.135 Btu/ft · h · °F (0.23 W/m² · K) and 0.47 Btu/lbm · °F (1959 kJ/kg · K) for thermal conductivity and specific heat, respectively. As a result, for preliminary predictions conducted before the intumescent model development, the VPI data were used. The VPI thermal properties provided reasonable agreement for the hypersonic aerothermal response data collected in several ground-test programs. When the independently measured virgin properties were used, the elevated temperature properties were backed out from only a backside temperature response, leaving uncertainty in the specific properties for the char, pyrolysis, and virgin materials. Additionally, due to the highly decomposing behavior of RX2390 at temperatures above 200°F (93.5°C), the temperature range of the data is limited.

When the laser thermal test results with embedded thermocouples and real-time radiography were used, it was possible to back out the necessary combination of thermal conductivity and specific heat, shown in Figs. 4 and 5, respectively, while incorporating the thermochemical decomposition and intumescence or conduction path growth. This represents a more rigorous approach for developing thermal properties of decomposing materials. This was accomplished through the use of transient density measurements and intumescence to validate the thermochemical decomposition predictions and ensure that more realistic conduction effects are isolated as opposed to assuming gross effective thermal properties to include decomposition. It was also determined that the independently measured thermal property data were suspect for the virgin material. As a result, vendor supplied virgin thermal properties were assumed for the intumescent model development. A comparison of the previously assumed properties obtained using laboratory thermal property data and convective aerothermal test data with only a backside temperature response is shown in Figs. 4 and 5. The fundamental importance of including the effects of intumescence can be seen on

conduction heat transfer. As shown in Fig. 4, thermal conductivity for the various decomposition states can significantly affect the applicability of heatshield analytic design models when not accounting for the relative intumescence behavior in low-shear aerothermal environments. The current approach in CMA is to utilize a weighting factor between fully charred and virgin states. A more appropriate method would be to attempt to understand the thermal properties for each phase of the decomposition process: virgin, pyrolysis, and fully charred. Note that the properties that have been determined are not necessarily the actual thermophysical material properties. They are simply the property values that yielded the best correlation of the thermal response data, given the modeling procedures and assumptions that have been made. This correlation was achieved through numerous iterations on thermal response for the three thermocouple locations within the material. The model was iterated until the transient density gradients, intumescence, thermal properties (thermal conductivity and specific heat), and corresponding in-depth thermal responses were accurately predicted through the material.

Elemental Composition

The elemental composition was determined for use in the thermochemical decomposition model defining the virgin material, char, and pyrolysis gases. The organic composition shown in Table 1 represents the pyrolysis gases passing through the char and mixing with the boundary-layer gases. The inorganic composition shown in Table 2 represents the fully charred material that remains after decomposition is complete. Percent weight of each element of organic

Table 1   Organic elemental composition

Element	wt%
Moisture	7.89
Carbon	52.3
Hydrogen	5.66
Nitrogen	<1.00
Oxygen	24.7
Sulfur	8.54

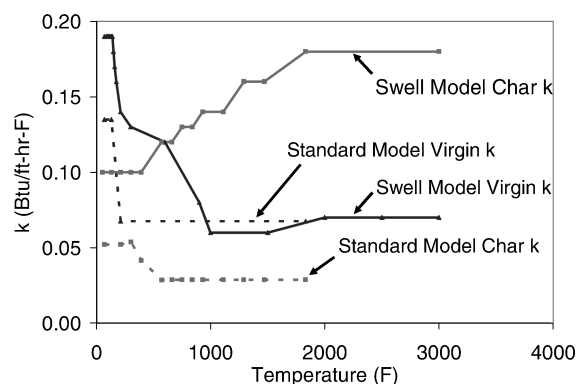**Fig. 4   Intumescent material thermal conductivity.**
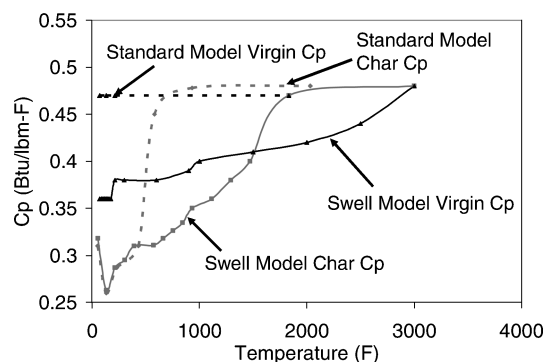
Fig. 5   Intumescent material specific heat.

Table 2   Inorganic elemental composition

Element	wt%
LOI[a]	54.51
Silica	30.37
Sodium	52.15
Sulfur	9.22
Aluminum	8.26

[a]Loss on ignition (organic constituents).
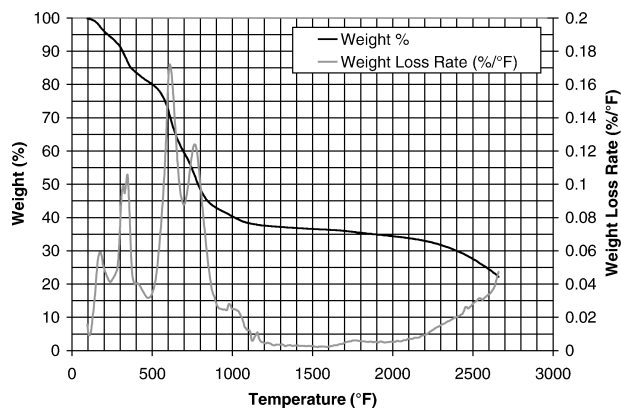
Fig. 6   TGA at 50°C/min.

and inorganic composition are required to determine the composition of the pyrolysis gases. Given the composition, the pyrolysis gas enthalpy is determined, assuming thermochemical equilibrium, with the ACE81 computer code.[13]

TGA

In addition to the characteristic thermal property measurements, thermodynamic decomposition (mass loss) as a function of temperature rise rate or heating rate was measured. These measurements are known as TGA and represent the outgassing that occurs when the temperature of a material exceeds reaction temperatures of the components. This information is used to define decomposition kinetics where specific coefficients are developed to model the intumescent heatshield material decomposition response.

Figure 6 provides the peak heating rate TGA data taken from tests conducted at two heating rates. Note that there are essentially four reactions that must be specifically modeled to ensure an accurate characterization of the internal decomposition. The peak reaction rate of 0.17%/°F for RX2390 occurs at approximately 600°F (316°C) with fairly substantial reactions occurring at even lower temperatures. The current Arrhenius model used for this research accounts for four reactions all occurring below 1500°F (816°C). A fifth reaction appears to be occurring above 2000°F (1094°C), but this is likely the result of small leaks within the TGA apparatus wherein the material sample is exposed to oxygen within the air. Because the thermal responses of interest for the missile applications investigated remained below 1500°F (816°C), it was determined that the current four reaction model was sufficient.

Intumescence Material Model Development and Validation

Overview

The two test facilities used to evaluate material performance experimentally represent a broad range of aerothermal environments with the intent of quantifying a variety of material behavior parameters. The test facilities utilized include the LHMEL for in-depth material thermodynamic response and the NASA Hot Gas Test Facility (HGTF) was for a realistic hypersonic convective environment response. These test facilities have capabilities to either reproduce or simulate some specific flight environment or effect. Importance has been placed on identifying the appropriate experimental facility and method to obtain the physical response necessary to separate and quantify phenomena of interest.

*Laser Test Facility and Intumescence Model Development*

The LHMEL is located in Dayton, Ohio, and maintains two carbon dioxide laser systems. LHMEL-1 is a 15-kW continuous wave electric discharge coaxial laser (EDCL) and the LHMEL-2 is a 150-kW continuous wave EDCL. The LHMEL-1 was used for this research effort. The laser beam is delivered and reflected to the target sample through the use of mirrors. The sample is attached to the holding fixture where the real-time radiography x-ray head is located. An exhaust system is in place to help evacuate pyrolysis gases during testing. This test facility provided a means of quantifying the transient intumescence and accompanying material decomposition decoupled from mechanical erosion due to shear. Through the use of these measurements and corresponding in-depth thermocouple data, the numerical model of the heatshield in-depth thermochemical behavior was developed and validated.

Test Setup

The test samples were attached to the holding fixture as shown in Fig. 7. This rectangular sample is 1.5×2.5 in. The laser beam was split and adjusted to impart the desired heat load on the sample. The radiography head was located above the sample looking down. The thermocouple plug (evident in Fig. 7) was located in the center of the sample. The thermocouple plug configuration is shown in Fig. 8 and involves the use of 36-gauge thermocouple wire and beads located at three different depths within the material. This provides for an in-line thermal response of the material as a function of time. The fixed x-ray reference plane was selected to be the 0.05-in. thermocouple bead location based on predicted thermal response and expansion and provided the in-depth density change and intumescence. Measurements are taken throughout the thickness of the sample but are centered about this reference plane because most of the response is expected to occur in this area.

Thermal Environment

Two heat fluxes were imparted to the samples representing Mach 4 and 5 type environments. These heat fluxes were imparted using 22 Btu/ft$^2 \cdot$ s (25 W/cm^2) and 66 Btu/ft$^2 \cdot$ s (75 W/cm^2), respectively, to induce the desired material thermal response. A 2-in.-diam beam width was used that minimized two-dimensional conduction effects at the sample edges.
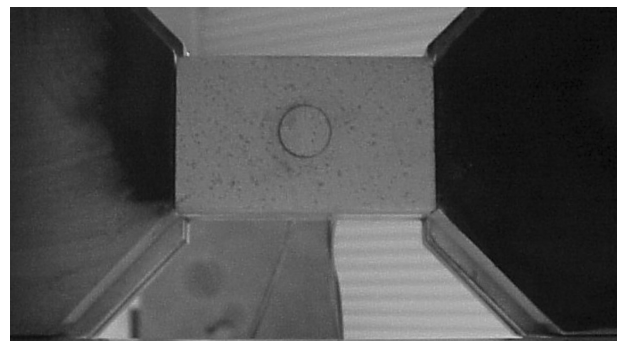
Fig. 7   Assembled sample configuration.
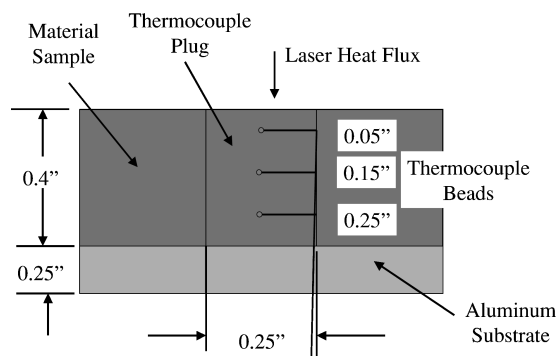
Fig. 8   Thermocouple plug configuration.

Posttest Results

Typical pre- and posttest photos of an RX2390 material sample are provided in Figs. 9 and 10. An example of the resulting real-time radiography used for defining transient density is provided in Fig. 11. Figure 11 shows the pre- and posttest positions of the relative heat-shield sample surface. Along with the radiography photographs, the LHMEL test facility digitized the transient densities as a function of position within the material. When the density through the thickness is qualitatively defined as a function of time and this response is correlated to the embedded thermocouple response, the density as a function of temperature and heat rate can be obtained. Figure 12 provides an example of the pre- and posttest density gradients through the material. The resulting weight and depth measurements are provided in Table 3. The weight measurement was obtained to validate the analytic model decomposition predictions of mass loss and in-depth decomposition. The pre- and posttest thickness measurements provide the total intumescence or swell, which can be used in conjunction with the real-time radiography to validate the intumescence model. The lower heating rate, test 1, resulted in approximately one-half of the total mass loss that the higher heating
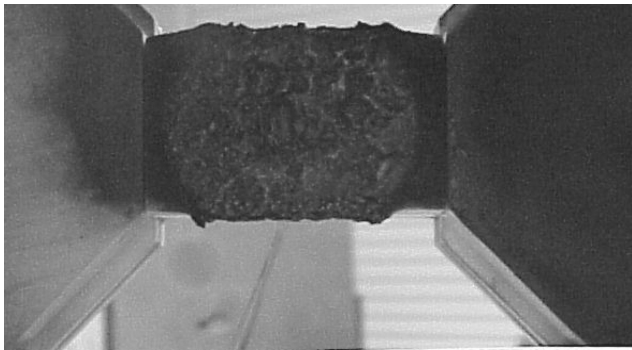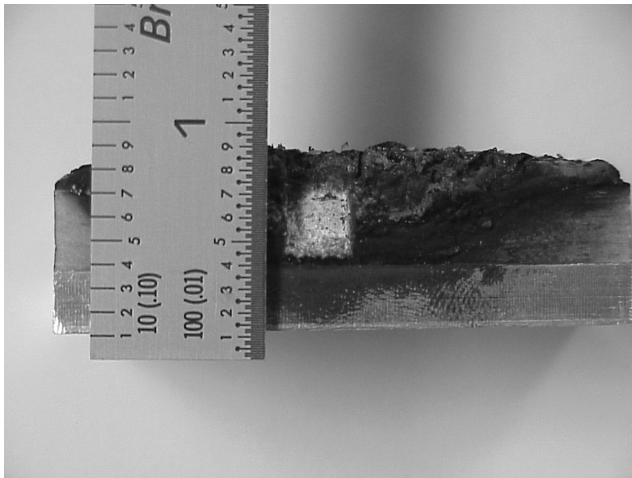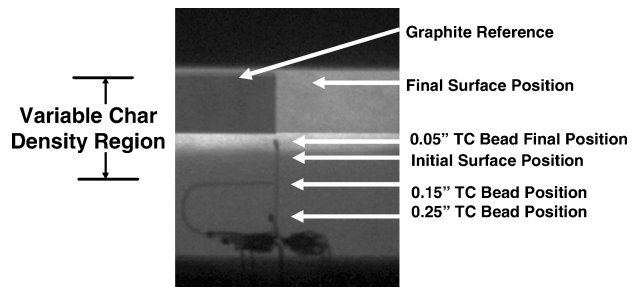
Table 3 Pre- and posttest measurements

	Test 1			Test 2		
Measurement	Pretest	Posttest	Change	Pretest	Posttest	Change
Weight, g	107.7	106.1	1.6	108.4	105.3	3.2
Thickness, in.	0.4	0.53	0.13	0.4	0.56	0.16
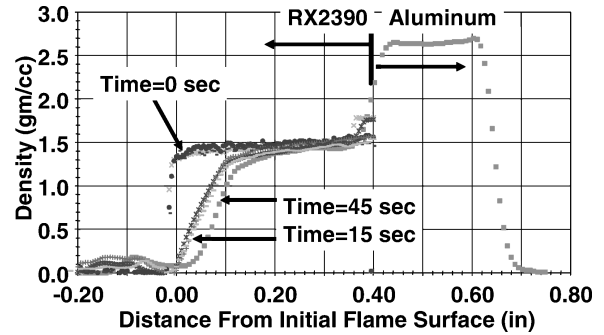
Fig. 12 Density gradient through sample.
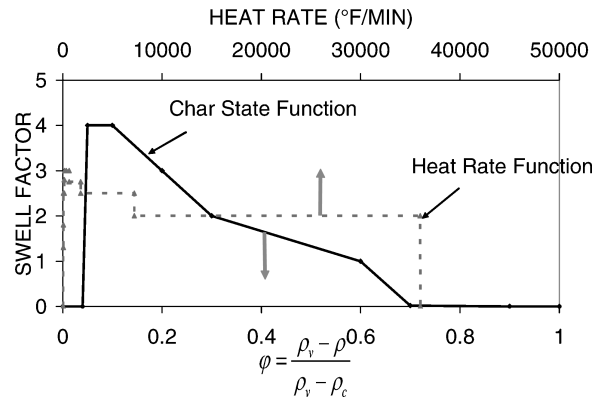
Fig. 13 Intumescence model functions.

rate test 2 experienced. However, the total intumescence was very similar for each test.

The baseline intumescence model was developed using the transient data collected on the two thermal tests conducted at LHMEL. Because two heating conditions were utilized and the material experiences a range of heating conditions in-depth, the heating rate dependency of intumescence could be determined. The model development was initiated by using the baseline intumescence model depending solely on decomposition state and comparing in-depth thermal responses at each of the thermocouple stations. The intumescence function was modified until the transient positions of heated surface, the 0.05-in. (0.13-cm) thermocouple bead, and in-depth heat-affected region (decomposition and virgin material interface) were matched. Matching rates, rather than final positions, provided an added fidelity to the analytic model. Once these intumescence trajectories were matched, the surface temperature and in-depth thermocouple response were correlated through modification of temperature-dependent properties. After a best match was selected for the relative thermal properties, the same analytic model was used to predict heatshield behavior in a realistic convective hypersonic high-altitude environment for which significant test data had been previously collected. Application to a convective environment quantified the usefulness of the model as well as the use of the LHMEL test facility to develop intumescence material properties. The analytic model was then used to predict thermal response for a supersonic sea-level (high-shear) convective environment to evaluate applicability for high-shear conditions. The results of these predictions provided indications of accuracy, applicability, and necessary model refinements for future research.

The resulting char state and heating rate dependency factors are provided in Fig. 13. These relationships represent the best fit

Fig. 9 Posttest material response.

Fig. 10 Sectioned view of material sample posttest.

Fig. 11 Example of real-time radiography.

combination for matching the LHMEL test conditions. However, through additional refinement and more accurate measurement of thermal properties for the various pyrolysis regions, these fits may be improved. Note that whereas these curves are considered a baseline, they do provide insight to the relative influence and trends associated with the intumescence phenomena. For example, when the char state factor is considered, it is evident that the majority of intumescence occurs in the initially pyrolysizing region where decomposition is below 32% weight loss. Therefore, the higher charred region experiences less intumescence. However, intumescence behavior is highly dependent on material formulation and flow chemistry. The use of different materials may lead to different intumescence properties. The lower intumescence of the charred region was again observed during the hypersonic convective thermal testing where it was seen that an insignificant level of additional swell was experienced between 200 and 300 s of testing. The additional 100 s of heating caused additional decomposition of the more fully charred regions but little additional intumescence. The addition of the heating rate factor was a result of realizing that with the use of only char state to quantify intumescence, a reasonable match of intumescence and in-depth thermal response could not be obtained for the wide range of thermal environments. An iterative process was used to obtain reasonable agreement with each LHMEL test condition. It was observed that below heating rates of approximately 72–180°F/min (40–100°C/min), very little intumescence occurred. When the transient radiography from tests 1 and 2 were used, the thermocouple station at 0.05 in. (0.13 cm) began moving when the heating rate reached and exceeded 180°F/min (100°C/min). The corresponding heating rate at the 0.05-in. (0.13-cm) station coupled with the transient radiography provided a means of determining the relative heating rate and temperature at which the thermocouple motion initiated. By adjustment of this heating rate dependency, the resulting intumescence factors shown in Fig. 13 were determined and provide a reasonable match for both laser thermal tests as well as the hypersonic convective thermal tests of test 3. It is possible that the heating rate dependency is a result of higher pyrolysis gas generation rates and limited gas transfer causing the localized material to puff up and initiate expansion, after which intumescence is reduced and is less dependent on heating rate. These concepts will be investigated in future research to expand the model applicability to a wider range of convective aerothermal and radiative environments.

The predicted transient intumescence as compared to data collected from the transient radiography is provided in Fig. 14. Identified in Fig. 14 are the surface position, in-depth decomposition, and the 0.05-in. (0.13-cm) thermocouple position as a function of time. This provides a comparison of the predicted and measured surface position and thermocouple position due to intumescence. The data were collected from video of x-ray data. Good agreement is obtained for the surface motion using the proposed intumescence properties. Some variation in data exists due to unevenness in the intumesced surface. A reasonable match was obtained for the in-depth decomposition, qualitatively assuming the ability to distinguish a 5% density loss in the radiography. The analytic model appears to overpredict the initial decomposition rate moving in-depth. This could be a result of uncertainties in thermal properties or inaccuracies in identifying the decomposition front from the radiography.
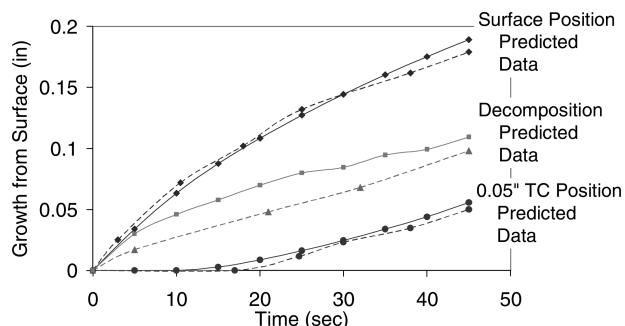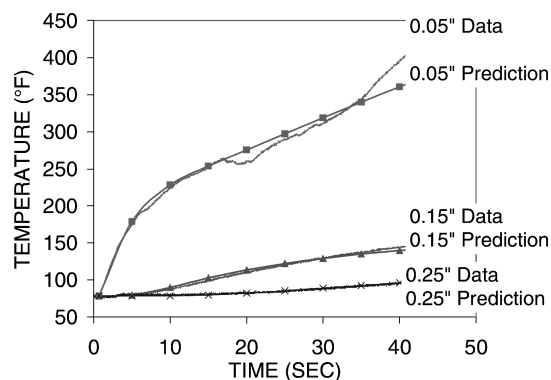

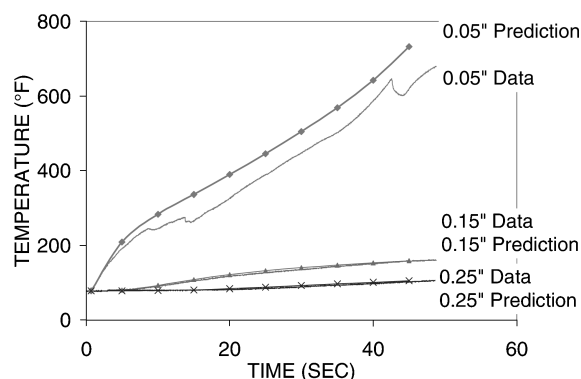**Fig. 15   Test 1, overall thermocouple response predictions vs data.**

Fig. 16   Test 2, overall thermocouple response predictions vs data.

The 0.05-in. (0.13-cm) thermocouple motion shows very good agreement, suggesting that not only total growth but also expansion rate is being modeled with reasonable accuracy. The initiation of thermocouple motion was noticeable for each of the tests at approximately 17–20 s with a measured temperature of 250–260°F (121–127°C). This response was identified for both the radiative heating environment imparted using the LHMEL test facility as well as the hypersonic convective environment imparted by the NASA HGTF. The thermocouple response appears to be disrupted at this time and temperature. This response provides an indication of intumescence and decomposition below the thermocouple.

Figure 15 provides a comparison of predicted temperatures with measured test data for the lower heating rate laser test, test 1, in which a heating rate of 22 Btu/ft^2 · s (25 W/cm^2) was imparted to the sample surface. Good agreement was obtained for surface temperature between the model predictions and optical pyrometer measurements with peaks of approximately 2000°F (1093°C). As can be seen in Fig. 15, a very good match was obtained for in-depth thermal response throughout the test until the thermocouple measurement and prediction intersect at approximately 34 s. However, because of movement of the thermocouple bead, quality of the measurement is degraded for times greater than 17 s. This effect becomes more significant later.

Note that a series of trades were performed during the thermal response predictions to define sensitivities to node size in the finite difference mesh resolution. Previous methods suggested node thicknesses on the order of 0.010–0.005 in. (0.025–0.013 cm) sufficiently captured the thermal gradient through the decomposing heatshield material. As a result of incorporating the intumescence model, it was determined that mesh resolution of 0.002–0.0005 in. (0.005–0.0013 cm) was required to define the thermal gradients accurately through the char and pyrolyzing regions. With additional statistically significant testing, better definition of thermodynamic response and corresponding sensitivities to mesh and material properties can be developed.

Figure 16 provides the in-depth thermocouple response predictions for the higher heating laser test, test 2, as compared to data. Although not shown in Fig. 16, the surface temperature measurement

Fig. 14   Intumescence behavior predictions vs data.

Table 4   Mass loss comparison of predictions and measurements

	Test 1			Test 2		
Measurement	Data	Prediction	Difference, %	Data	Prediction	Difference, %
Posttest weight, g	1.60	1.21	32	3.2	1.40	220
Modified model weight, g	1.60	1.4	13	3.2	2.6	19
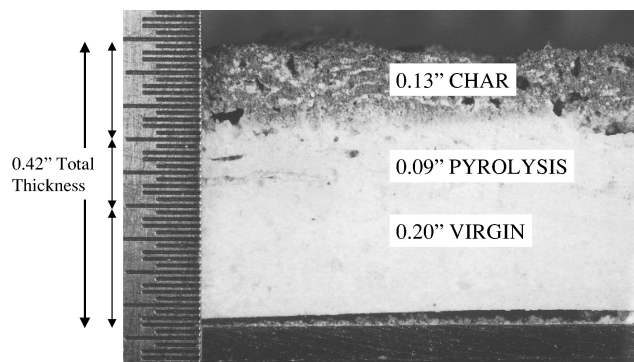
Fig. 17   Sectioned view of in-depth decomposition.

and predictions were in good agreement with peaks of approximately 2700°F (1482°C). As can be seen, at approximately 17 s, the measured thermal response drops and recovers its increasing slope. As a result, the 0.05-in. (0.13-cm) thermocouple response does not truly represent the 0.05-in. (0.13-cm) layer within the decomposing material. Therefore, the temperature at this location is not accurately measured and prediction should be higher than the data throughout the remainder of the test. Because significant intumescence did not occur at the 0.15-in. (0.38-cm) and 0.25-in. (0.64-cm) thermocouple positions, the thermal response measurements are smooth. For the assumed pyrolyzing region thermal properties and intumescence factors, a reasonable match is obtained for these thermocouple measurements. With additional iteration of thermal properties, a better match could be obtained throughout the test. However, the primary goal of this effort is to develop analytic models to account for intumescence. Future efforts will be directed toward better quantifying in-depth thermal properties as a function of decomposition and temperature. The ability to model intumescence also provides a means of more accurately decoupling and quantifying thermal properties of an intumescing material.

Table 4 contains the predicted mass loss results as compared to the measured values. The initial predictions do not include observed two-dimensional effects due to conduction and increased decomposition outside the laser beam diameter. The second set of predictions was used to attempt to account for this effect and, as expected, brought predictions and data within reasonable accuracy. Note that the TGA model was developed for a maximum temperature of approximately 1500°F (816°C). For the higher heating rate where surface temperatures approached or exceeded 2700°F (1482°C), surface reactions may have occurred and resulted in additional material removal.

Hypersonic Convective Intumescence Predictions and Data

The resulting predicted thermal response and intumescence agreement obtained for the two laser heating tests led to the application of the analytic model and corresponding intumescence properties to the hypersonic convective heating test environment. The Mach 6 and 8 environments of interest were represented by constant cold wall heat flux values of 6 and 8.5 Btu/ft$^2 \cdot$ s (6.8 and 9.6 W/cm^2), respectively. The total temperatures delivered by the test facility were 2300°F (1260°C) for the Mach 6 condition and 3000°F (1649°C) for the Mach 8 condition. For the Mach 6 test case, the surface temperature response reached approximately 950°F (510°C), with the average backside thermal response reaching 160°F (71°C). The resulting in-depth thermochemical decomposition is shown in Fig. 17 for the Mach 6 test condition. Note that

Table 5   Ablation measurements for Mach 6 test[a]

Measurement	Material, in. (cm)
Pretest thickness	0.3 (0.76)
Char depth	0.13 (0.33)
Pyrolysis depth	0.09 (0.23)
Virgin material depth	0.2 (0.5)
Posttest thickness	0.42 (1.07)
SHOA total ablation	0.1 (0.25)

[a]Average intumescence is 120%.
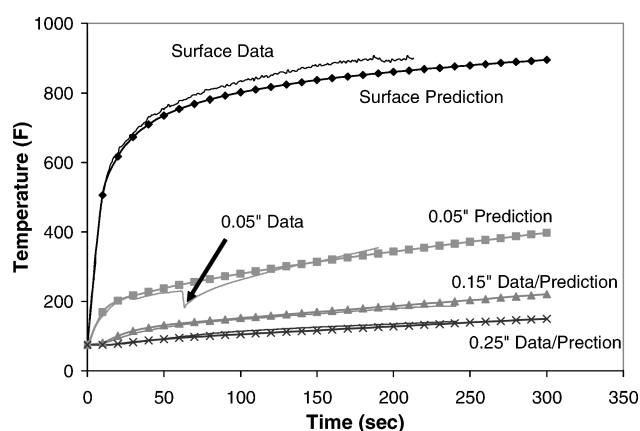
Fig. 18   Test 3, overall thermocouple response predictions vs data.

a significant level of internal decomposition occurred during the test. The material maintained a relatively strong char. Table 5 provides a summary of decomposition as measured after the test. The value of total ablation for the test sample was 0.10 in. (0.25 cm) (as defined by the SHOA procedure). This highly decomposing material provided significant thermal performance in the form of limiting backside temperature rise when compared to low-density, low thermal conductivity materials. Note that where volume constraints are more important than weight constraints, intumescing material performance should be investigated. When weight constraints are equal or more severe than volume constraints, decomposing materials become less attractive. However, simply assuming the need for low-density low thermal conductivity materials can greatly restrict the potential identification of superior heatshield materials.

The predicted thermal response and intumescence agreement obtained for the two laser heating tests led to the application of the analytic model and corresponding intumescence properties to the hypersonic convective heating test environment. The resulting predictions as compared to data are provided in Figs. 18 and 19. As can be seen in Fig. 18, the surface temperature prediction matches reasonably well for the initial 50 s. However, the curves deviate slightly, suggesting the need for additional understanding of the char state density and thermal properties. Good agreement is obtained for the in-depth thermal response matching both magnitude and slope. This was one of the primary goals of developing the intumescence model. The necessity of better predicting the heat transfer and resulting thermal response slope was evident when applying the analytic model to longer heating times seen in actual flight conditions. Original model predictions gave significantly different slopes for the test time and would actually predict excessively higher thermal response and resulting excessive heatshield requirements for continued heating. The same thermocouple event (discontinuity at approximately 60 s) can be seen as in the laser tests at a similar decomposition state and
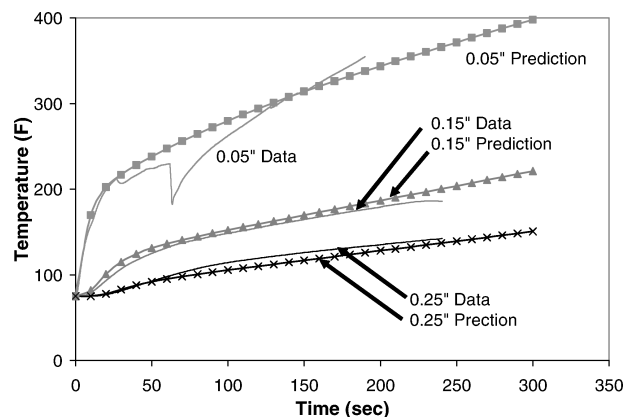
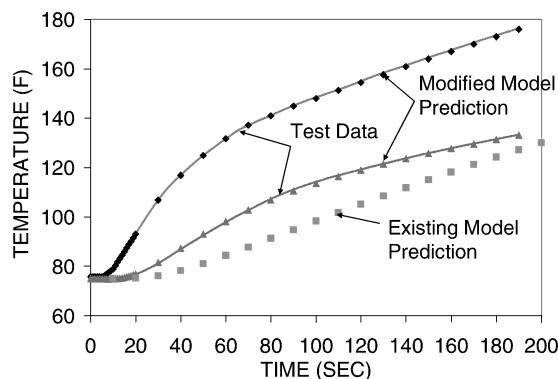Fig. 19 Test 3, in-depth thermocouple response predictions vs data.

Fig. 20 Test 3 earlier and new model prediction comparisons.

temperature. When in-depth heating rate predictions and measured thermal response are used, an indication of motion and onset of decomposition was obtained. Similar to the lower heating rate laser test analytic results, the predicted 0.05-in. (0.13-cm) thermal response intersects the measurement and suggests that after the intumescence region is initiated and the thermocouple bead detaches from the surrounding material, the quality of the thermal response is questionable. Figure 19 shows the same results with the scale changed to better illustrate the comparison of the predicted and measured response. Figure 20 provides a comparison with the previous model predictions (using the standard CMA properties identified earlier in Figs. 4 and 5) and shows the improvement obtained by modeling intumescence. The in-depth thermocouple responses are shown along with the previous and new model predictions. As can be seen, the previous model predictions gave thermal response slopes significantly different than test data. This model, using the standard CMA method, was the best fit that could be obtained (with only backside temperature data) and suggested the need for the more detailed intumescent modeling capability. The test data indicated a decreasing slope or plateau and gradual increase in temperature at the 0.25-in. (0.64-cm) thermocouple position. The previous model predicted a relatively constant temperature rise rate, suggesting an underprediction for early test times and an overprediction for longer test times. (Note that the model had been developed to best match results at the end of the 300-s test.) The impact of the slope can be expressed as a function of predicted thermal protection requirements for flight-test times longer than those experimentally induced. A significant increase in thermal protection and corresponding weight would be required, adversely affecting system performance. However, the new model predictions clearly demonstrate a better match with the transient thermal response of the in-depth thermocouples. By more accurate prediction of the transient thermal response, the model applicability is extended to actual flight environments, providing accurate thermal response and heatshield predictions for a range of aerothermal environments, flight times, and geometric configurations.

Summary

In summary, the objective of this research was to initiate the first step of incorporating the effects of intumescence on the in-depth energy balance as defined in the CMA. Previous methods to account for this effect on heat transfer in decomposing materials included effective thermal properties and an attempt to correlate a classical thermal expansion model. These approaches were limited because they did not attempt to model the phenomena actually occurring but instead attempted to lump unmodeled phenomenon into a single term. Some of the phenomena that must be specifically modeled include pyrolysis gas generation, intumescence, temperature- and density-dependent thermal properties, and decomposition energies. The addition of modeling intumescence provided a previously unavailable capability to account for material expansion during thermochemical decomposition and its relative effect on in-depth conduction. For external thermal protection systems exposed to extreme thermal environments, a significant level of thermal performance can be attributed to the conduction path growth and resulting reduction in heat transfer to temperature critical substructures. The intumescence model was initially derived through the use of high-enthalpy aerothermal environments with minimal aerodynamic shear contribution. These conditions induced sufficient intumescence to identify specifically the relative effects on in-depth heat transfer through the use of embedded thermocouples. Real-time radiography provided the method of validating in-depth intumescence as a function of decomposition state. Coupling the embedded thermocouple data with intumescence provided for the heating rate dependency. The analytic approach included a mathematical model coupled to a material property table of intumescence as a function of char state and heating rate. The resulting model was then successfully applied to a low-shear hypersonic aerothermal environment in which significant thermal and intumescence data was previously obtained. Intumescence and in-depth thermal response predictions showed good agreement with measured data and further validated the model's application to a hypersonic convective aerothermal environment.

Following is a list of recommended future research that would add significantly to the analytic modeling capability of heatshield design. The current modifications to CMA of intumescence could be used as the foundation for adding these capabilities.

1) Mechanical shear: It is recommended that the ability to model mechanical shear removal of material as a function of char state and char strength be incorporated into the CMA modeling approach. This additional phenomenon would complete the current goal to enhance the CMA code and accommodate much of the heatshield design and optimization requirements for current supersonic and hypersonic thermal protection systems.

2) Intumescence model refinement: Additional research is recommended to refine the intumescence model. These efforts should be devoted to refining the understanding of intumescence and validating the analytic approach for a wide range of aerothermal environments. These environments should include commercial building insulation designs where a significant benefit in optimization could be realized. The LHMEL test facility should be utilized for a statistically significant number of test samples to better quantify in-depth decomposition, intumescence, and thermal response.

3) Test facility measurement capabilities, real-time radiography: It is also recommended that research be devoted to develop real-time radiography measurement capability that can readily be adapted for use at any aerothermal test facility. This capability coupled to the use of embedded thermocouples significantly increases the understanding of material response and can greatly reduce the overdesign methodology and increase system performance through optimization.

4) Test facility measurement capabilities, pyrolysis gas injection rates and species: Methods of quantifying pyrolysis gas injection rates and mechanical erosion rates should be developed and incorporated into aerothermal test facilities. These results could be used to validate the transient thermochemical decomposition and corresponding mass loss predictions for various heatshield materials. Of additional interest is the ability to measure the individual mass injection species and injection rates within the boundary-layer flow,

as well as the resulting boundary-layer thickness increase. These measurements would greatly enhance the analytic model validation and increase the model application.

5) Transient skin friction and hot wall effects: Coupled to the measurements and analytic model enhancements just suggested is the ability to measure skin friction on intumescing and ablating heatshields under aerodynamic heating conditions. Although this was specifically addressed during the NASA HGTF aerothermal test program, this capability should be developed for higher-shear and -enthalpy test facilities such as the U.S. Naval Air Warfare Center T-Range, U.S. Air Force Holloman High Speed Test Track, Arnold Engineering Development Center, as well as other aerothermal test facilities. This ability would provide the transient hot wall effects and external heatshield influence on the aerodynamic drag models commonly developed in cold flow wind tunnels.

Acknowledgments

References

[1]Rohsenhow, W. M., and Hartnett, J. P., *Handbook of Heat Transfer*, McGraw–Hill, New York, 1973, Secs. 16-34 and 16-39.

[2]Russell, G. W., Rembert, M., Strobel, F. A., and Jaul, W. K., "Development of High Performance Thermal Protection Systems for Hypersonic Missiles," *Proceedings, RLV/SOV Airframe Technology Review*, NASA Langley Research Center, Hampton, VA, 2002, p. 4.14.

[3]"Aerotherm Charring Material Thermal Response and Ablation Program (CMA87S)," Acurex Rept. UM 87-13/ATD, Aerotherm Div., Acurex Corp., Mountain View, CA, Nov. 1987.

[4]Schlichting, H., *Boundary Layer Theory*, McGraw–Hill, New York, 1979, p. 24.

[5]Doyle, C. D., "Kinetic Analysis of Thermogravimetric Data," *Journal of Applied Polymer Science*, Vol. 5, No. 15, 1961, pp. 285–292.

[6]Koo, J. H., "Thermal Characteristics Comparison of Two Fire Resistant Materials," *Journal of Fire Sciences*, Vol. 15, No. 3, 1997, pp. 203–221.

[7]Shih, Y. C., Cheung, F. B., and Koo, J. H., "Theoretical Modeling of Intumescent Fire-Retardant Materials," *Journal of Fire Sciences*, Vol. 16, No. 1, 1998, pp. 46–71.

[8]Reynolds, R. A., Russell, G. W., and Nourse, R. W., "Ablation Performance Characterization of Thermal Protection Materials Using a Mach 4.4 Sled Test," AIAA Paper 92-3055, June 1992.

[9]Moyer, C. B., and Rindal, R. A., "An Analysis of the Coupled Chemically Reacting Boundary Layer and Charring Ablator, Part II—Finite Difference Solution for the In-Depth Response of Charring Materials Considering Surface and Energy Balances," Aerotherm Rept. 66-7, Pt. 2, Vidya Div., ITEK Corp., Palo Alto, CA, Nov. 1968; also NASA CR-1061, Nov. 1968.

[10]Russell, G. W., "Analytic Modeling and Experimental Validation of Intumescent Behavior of Charring Heatshield Materials," Ph.D. Dissertation, Dept. of Mechanical and Aerospace Engineering, Univ. of Alabama, Huntsville, AL, June 2002, p. 45.

[11]Reynolds, R. A., Nourse, R. N., and Russell, G. W., "Aerothermal Ablation Behavior of Selected Candidate External Insulation Materials," AIAA Paper 92-3056, 1992.

[12]Russell, G. W., "Evaluation of Decomposition Kinetic Coefficients for a Fiber-Reinforced Intumescent Epoxy," AIAA Paper 93-1856, June 1993.

[13]"Aerotherm Chemical Equilibrium Computer Program (ACE81)," Acurex Rept. UM 81-11/ATD, Aerotherm Div., Acurex Corp., Mountain View, CA, Aug. 1981.

T. Lin
Associate Editor